

# Mathematical Investigation of Flow and Heat Transfer in Nanofluid over a Radially Stretching Surface with Joule Heating

Ameer Hamza, Azeem Shahzad

*“Department of Mathematical Sciences Faculty of Basic Sciences & Humanities University of Engineering and Technology Taxila Pakistan”*

---

## **Abstract**

*The aim of this investigation is to determine the flow and heat transfer of ethylene-glycol based fluid with aluminum oxide nanoparticles over a radially stretching surface. Specifically, we will investigate how various shapes of nanoparticles impact the flow and heat transfer in the existence of Joule heating. Governing nonlinear differential equations are simplified by similarity transformation and numerical result will be found by BVP4C. Graphs and tables will be drawn to determine the influence of various physical parameters on temperature and velocity profiles.*

**Keywords:** Radially Stretching surface, Magneto hydrodynamic (MHD),  $Al_2O_3$  nanoparticles

---

Date of Submission: 13-10-2024

Date of acceptance: 28-10-2024

---

## **I. Introduction**

Nanofluids are suspensions of nanometer-sized solid particles or fibers (with average size below 100nm) involving a base fluid. There are instances where several kinds of nanoparticles are employed these days. These nanoparticles-sized are essential for managing the diverse thermophysical characteristics of the numerous related flows. The majority of practical fluids, including ethylene glycol, kerosene oil, motor oil, and water are poor heat conductors. The main causes of this include low thermal conductivity and various thermal characteristics. Nanoparticles are introduced to the base fluids in order to address this issue and enhance the thermal characteristics of these flows. Materials that are frequently used to make nanoparticles include oxide ceramics ( $Al_2O_3$ , CuO,  $TiO_2$ ,  $SiO_2$ ), and chemically stable metals (Al, Au, Ag, and Cu).

Nanofluids come in various types that are based on the particles they contain. These types include metallic nanofluids, which contain metallic nanoparticles like copper, gold, silver, and aluminum; oxide nanofluids, which contain oxide nanoparticles like titanium dioxide, alumina, and zinc oxide; carbon nanofluids, which contain carbon-based nanoparticles like carbon nanotubes and graphene; and polymer nanofluids, which contain polymer-based nanoparticles like polystyrene and polyethylene glycol. Additionally, the shape of the nanoparticles in a nanofluid can vary and may include spherical, rod-shaped, platelet-shaped, or other shapes such as triangular, cubic, and tetrahedral, depending on the specific application requirements.

Industry fields such as developed, health carefulness, transportations, energy and nuclear system have advanced with quick industrial development in the past few years. One of the vital elements has been pragmatic in such industries is cooling/heating process, which can be boosted by using nanofluid technology. Furthermore, a throughout examination of the flow over the radially extending surfaces of the nanofluids has several important industrial applications, such as the creation of plastic films, glass, paper, and crude oil refinement. Furthermore, a number of academics have focused their latest analyses on the use of nanotechnology because of the outstanding electrical, optical, and chemical behavior that nanoparticles display, as well as their Brownian motion and thermophoresis features. These characteristics make the nanoparticles popular in applications such as microelectronics, imaging, energy-based research, catalysis, and environmental and medical fields. Either metals or non-metals make up these particles. Furthermore, recent studies have made it possible to include nanoparticles into heat transfer fluids. Nanofluid was firstly utilized by Choi and Eastman [1]. Nowadays this technology is widely used. Nanofluid is now being developed for medical applications. Nanofluid has a major implication in many industries from the past decades up to now. Buongiorno [2] developed a mathematical model for convective transport of nanofluid by considering seven slip mechanisms. Ariel [3] investigated the slip effects on an axisymmetric flow over a radially stretching sheet and obtained exact and numerical solution. Mustafa et al. [4] examine axisymmetric flow of nanoliquid past a radially stretching surface. A thorough examination was conducted of the combined effects of heat radiation, Brownian motion, magnetic field, and variable viscosity on the boundary layer flow of nanofluid past a surface that is extending radially by Makinde

et al. [5]. An analysis has been conducted on the effect of Joule heating on the nanofluid flow via a permeable duct by Li et al. [6]. Hayat et al. [7] examined the MHD flow of a nanofluid caused by a spinning disc and the slip effect. Additionally, they looked at how a stretched sheet affected the creation and absorption of heat in Oldroyd-B nanofluid. Sarkar et al. [8] set the fluid model results over two extended rotating discs to the test. Gangadhar et al.

[9] inspected structures of irregular free variable movement nanofluid flow on a extended surface using a spectrum coping method. Sandeep et al. [10] investigated effect of nonlinear radiation on MHD flow of hybrid nanoliquids with heat source impact. Vinita and Poply [11] examined the MHD slip fluid flow of a nanofluid towards a stretched surface when there is an outer velocity or free stream velocity. Vinita et al.

[12] examined MHD fluid flow on a non-linear stretching surface under changing slip circumstances. Zaher et al. [13] studied the (electro-osmotic forces) EOF over the boundary layer flow induced by Williamson nanoliquid with micro-organisms in a non- Darcy medium. Das et al. [14] set the fluid model results over two stressed rotating discs to the test. Gangadhar et al. [15] studied irregular free variable movement characteristics nanofluid flow on a overextended surface employing a spectrum coping technique. Jiang et al. [16] utilized a 3D computer model to examin nanofluid thermal capillary flow around a gas bubble. This study considers various critical physical parameters as it investigates the impact of nanoparticle shape on the nanoliquids of Al<sub>2</sub>O<sub>3</sub> nanoparticles with silicon(Si) oil base fluid on a radially stretched rotating disc. Patil [17] examined how nonlinear radiation affected the hybrid nanofluids MHD flow while accounting for the heat source impact. Patil [18]–[20] worked on several geometries with noteworthy physical properties and published several publications about them.

Butt et al. [22] have planned heat transfer past a radially stretching exhausting different fluids. Soomro et al. [23] studied the nonlinear radiation and heat generation/absorption of a nanofluid at the stagnation point of a moving sheet. Nadeem et al. [24] deliberated the nonlinear extending sheet to sightseen the characteristics of heat transfer in the occurrence of three various nanoparticles, such as TiO<sub>2</sub>, Cu, and Al<sub>2</sub>O<sub>3</sub>. Khan et al. [25] investigated the 3D unsteady nanofluid movement of carbon nanotubes in presence of thermal slip & velocity. It is evident from literature review that not a single attempt has so far been communicated with respect to effects of shape on flow and heat transfer of nanofluid in the presence of joule heating along radially stretching sheet. Current study will fulfill this gape. The main proposed of this work is to analyses the impact of different-shape nanoparticles like (brick, sphere, platelets, Blade, cylinder) and joule heating effects of (Al<sub>2</sub>O<sub>3</sub>) nanoparticle with base fluid ethylene glycol over a radial extending sheet along convective boundary conditions with an external magnetic field present. The next part will describe the modelling of the whole phenomenon and the technique used to solve it.

### Nomenclature

$\mu_f$	Dynamic viscosity of base fluid	$\rho_f$	Density of base fluid
$\rho_s$	Density of nanoparticles	$M$	Magnetic Parameter
$(\rho C_p)_{nf}$	Heat capacitance of nanofluid	$E_c$	Eckert number
$S$	Unsteadiness parameter	$Pr$	Prandtl number
$k_{nf}$	Thermal conductivity of nanofluid	$K$	Slip Parameter
$\eta$	Similarity Variable	$Re$	Reynolds number
$\Psi$	Stream function	$k_f$	Thermal conductivity of base fluid
$\phi$	Solid volume fraction	$C_f$	Skin friction coefficient
$\rho_{nf}$	Density of nanofluid	$\mu_{nf}$	Viscosity of nanofluid

**Problem Formulation**

In existence of joule heating at a radially stretching surface, we considered heat transmission and boundary layer flow of nanofluid in this problem. Where we assume radially stretching velocity of surface  $U$  & a constant magnetic field of strength  $B_0$  is applied normally to the surface. In this case, the  $z$ -axis is normal to the  $r$ -axis, and the  $r$ -axis is chosen in the direction of sheet motion. Let  $T = T(r, z)$  be the temperature of nanofluid and  $u = u(r, z)$  and  $w = w(r, z)$  be the components of velocity along the  $r$  and  $z$  coordinate axis. The sheet is extend in the direction of  $r$  with velocity  $U = cr$  such that  $r$  -directional velocity component varies linearly along it and  $z$  - axis is normal to the surface. Surface temperature is considered as  $T = T_w$ .

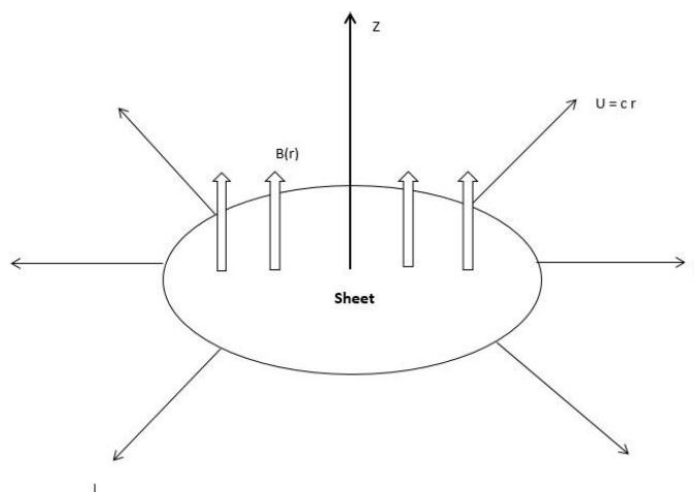


Figure1. Graphical representation of the radially stretching disc.

Based on the stated assumptions the governing equation for Momentum, Mass and Energy can be written as follows.

$$\frac{\partial u}{\partial r} + \frac{u}{r} + \frac{\partial w}{\partial z} = 0, \tag{1}$$

$$\frac{\partial u}{\partial t} + u \frac{\partial u}{\partial r} + w \frac{\partial u}{\partial z} = \frac{\partial^2 u}{\partial z^2} + \frac{\sigma_{nf} B^2 u}{\rho_{nf} \nu_{nf}}, \tag{2}$$

$$u \frac{\partial T}{\partial r} + w \frac{\partial T}{\partial z} = \frac{k_{nf}}{(\rho C_p)_{nf}} \frac{\partial^2 T}{\partial z^2} + \frac{\mu_{nf}}{(\rho C_p)_{nf}} \left( \frac{\partial u}{\partial z} \right)^2 + \frac{\sigma_{nf} B^2 u^2}{(\rho C_p)_{nf}}, \tag{3}$$

Related to the BC's [26], [27].

$$U \rightarrow 0, \quad T \rightarrow T_\infty \quad \text{as} \quad z \rightarrow \infty,$$

$$u = U + Av \frac{\partial u}{\partial z}, \quad T = T_w \quad \text{at} \quad z = 0$$

Physical parameters are given as [30]

$$\alpha_{nf} = \frac{K_{nf}}{(\rho C_p)_{nf}}, \quad \rho_{nf} = (1 - \phi)\rho_f + \phi\rho_s,$$

And thermal conductivity ratio is

$$\frac{k_{nf}}{k_f} = \frac{K_s + (mm-1) \cdot k_f + (mm-1)(k_s - k_f) \cdot \Phi}{k_s + (mm-1) \cdot k_f - (k_s - k_f) \cdot \Phi}$$

$$\frac{\mu_{nf}}{\mu_f} = (1 + A_1 \Phi + A_2 \Phi^2), \frac{\sigma_{nf}}{\sigma_f} = (1 - \Phi) \sigma_f + \Phi \sigma_s$$

Using similarity transformations [28] mentioned below, we will obtain dimensionless variables, which will be utilized to make the system dimensionless, following dimensionless variables will be used

$$\theta(\eta) = \frac{T-T_o}{T_\infty-T_o}, \quad \eta = \frac{z}{r} Re^{\frac{1}{2}}, \quad \psi = r^{-2} U Re^{-\frac{1}{2}} f(\eta), \quad (4)$$

Here  $\eta$  is independent variable and  $\psi$  is the stokes theorem function,

$$w = \frac{1}{r} \frac{\partial \psi}{\partial r}, \quad u = -\frac{1}{r} \frac{\partial \psi}{\partial z}$$

So the velocity component are

$$w = -2URe^{-\frac{1}{2}} f(\eta), \quad u = U f'(\eta). \quad (5)$$

Using the established set of similarities Equations (2) and (3) are reduced to a set of ordinary differential equations with boundary conditions.

$$f''' = \frac{1}{\epsilon_1} (f'^2 - 2ff'' + \epsilon_3 Mf'). \quad (6)$$

$$\theta''(\eta) = -\frac{Pr}{\epsilon_2} [2f(\eta)\theta'(\eta) + \epsilon_4 Ec f''^2(\eta) + \epsilon_5 Ec M f'^2]. \quad (7)$$

BC's are,

$$f(0) = 0, f'(\infty) = 0$$

$$f'(0) = 1 + K f''(0), \theta(0) = 1, \theta(\infty) = 0. \quad (8)$$

As,  $Re = \frac{rU}{\nu_f}$  is Reynold parameter,  $Pr = \frac{(\rho C_p \nu)}{k_f}$  is Prandtl parameter,  $K = A \sqrt{\frac{\nu_f U}{r}}$  partial slip parameter,  $Ec = \frac{U^2}{C_p(T_w - T_\infty)}$  is the Eckert number and  $\epsilon_1, \epsilon_2, \epsilon_3, \epsilon_4, \epsilon_5$  are constants which are defined as,

$$\epsilon_1 = \frac{1 + A_1 \Phi + A_2 \Phi^2}{(1 - \Phi + \Phi (\frac{\rho_s}{\rho_f}))}, \quad \epsilon_2 = \frac{\frac{k_{nf}}{k_f}}{(1 - \Phi + \Phi (\frac{\rho C_p \nu_s}{\rho C_p \nu_f}))}, \quad \epsilon_3 = \frac{(1 - \Phi + \Phi (\frac{\sigma_s}{\sigma_f}))}{(1 - \Phi + \Phi (\frac{\rho_s}{\rho_f}))}$$

$$\epsilon_4 = \frac{(1 - \Phi + \Phi (\frac{\sigma_s}{\sigma_f}))}{(1 - \Phi + \Phi (\frac{\rho C_p \nu_s}{\rho C_p \nu_f}))}, \quad \epsilon_5 = \frac{1 + A_1 \Phi + A_2 \Phi^2}{(1 - \Phi + \Phi (\frac{\rho C_p \nu_s}{\rho C_p \nu_f}))}$$

Since shear stress and heat transfer rate can be defined as,

$$Cf_r = \frac{\tau_w}{\rho(U)^2}$$

$$Nu_r = \frac{r q_w(r)}{k_f [T_w - T_\infty]}$$

where  $\tau = \mu \frac{\partial u}{\partial z} \Big|_{z=0}$  and  $q_w(r) = -k \frac{\partial T}{\partial z} \Big|_{z=0}$ , are wall heat flux and shear stress

$$Re^{\frac{1}{2}} C_f = (1 + A_1\phi + A_2\phi^2)f''(0) \tag{9}$$

$$Re^{-\frac{1}{2}} Nu = -\frac{K_{nf}}{K_f} \theta'(0) \tag{10}$$






Equations (9) and (10) are the skin fraction-coefficient ( $Re^{\frac{1}{2}} C_f$ ) and Nusselt number ( $Re^{\frac{1}{2}} Nu$ ).

The values of specific heat capacity, thermal conductivity, density, and electrical conductivity of ethylene glycol and  $Al_2O_3$  (alumina) nanoparticles at the different temperatures are shown in Table 1. Table 2 lists down the viscosity and form factor for different shapes of nanoparticles such as the platelet, cylinder, blade, brick and spherical nanoparticles.

**Table 1:** Thermo physical Properties (Characteristics) of  $Al_2O_3$  nanoparticles. [21]

Nanoparticles /Base Fluid	Specific Heat $C_p(J/kg K)$	Thermal Conductivity $K(W/mK)$	Density $\rho(kg/m^3)$	Electric Conductivity $(S/m)$
$Al_2O_3$	765	40	3970	16.5
Ethylene Glycol	2430	0.253	1115	3.14

**Table 2:** Viscosity and shape factor values nanoparticles [26]

Nanoparticles	Platelet	Cylinder	Blade	Brick	Sphere
Parameters					
$A_1$	37.1	13.5	14.6	1.9	2.5
$A_2$	612.6	904.4	123.3	471.4	6.5
$m$	5.72	4.82	8.26	3.72	3.0

**Numerical Solution**

This problem is solved numerically; the BVP4C method is employed as per the references provided [29]. It is specifically appreciated by researchers for its main characteristics, especially for solving singular BVP4C, and for the direct acceptance of not only the two-point but also the multi-point BVPs with high accuracy and convergence rate and, therefore, low error. To use the above method the third order ordinary differential Equation (6) and the second order ordinary differential Equation (7) has been transformed to first order differential equations.

$$\begin{aligned}
 f &= y_{(1)}, \\
 f' &= y'_{(1)} = y_{(2)}, \\
 f'' &= y'_{(2)} = y_{(3)}, \\
 f''' &= y'_{(3)} = \frac{1}{\epsilon_1} * ((y_{(2)})^2 - 2y_{(1)} * y_{(3)} + \epsilon * M * y_{(2)}), \tag{11}
 \end{aligned}$$

$$\begin{aligned}
 \theta &= y_{(4)}, \\
 \theta' &= y'_{(4)} = y_{(5)}, \text{ and} \\
 \theta'' &= y'_{(5)} = \frac{Pr}{\epsilon_2} * (-2 y_{(1)} * y_{(5)} - E * \epsilon * (y_{(3)})^2 - \epsilon * Ec * M * (y_{(2)})^2) \tag{12}
 \end{aligned}$$

Boundary conditions are

$$\begin{aligned}
 y_{(2)}(\infty) &= 0, y_{(2)}(0) = 1 + K * y_{(3)}(0), \\
 y_{(1)}(0) &= 0, y_{(4)}(0) = 1, y_{(4)}(\infty) = 0. \tag{13}
 \end{aligned}$$

**Result and Discussion**

In this segment, numerical outcomes of the skin-friction number and Nusselt parameter are recorded in tables and represent in graphs. So dimensionless mathematical model that describes the problem, including the governing equations, boundary conditions, and dimensionless parameters. The BVP-4C approach used to solve dimensionless mathematical model numerically for different sets of parameter values. This involves discretizing the equations and applying appropriate boundary conditions. . Notice the mainly important numbers such as *Ec* Eckert number, *M* magnetic parameter, *K* partially slip parameter and  $\phi$  solid volume fraction, *Pr* Prandtl number. Also a detail outcome for heat transfer coefficient and as well skin friction. Choose a range of values for each significant parameter (*M*,  $\phi$ , *Ec*, *K*, and *Pr*) that we want to investigate. It is advisable to select a broad range to observe the full behavior of the system. Analyze and interpret the results obtained from the plots and tables. Discuss the trends and observations related to the effect of each parameter on the flow and temperature fields.

This study, we investigate a mathematical model for 2D boundary layer flow of nanofluids with various shapes of Al<sub>2</sub>O<sub>3</sub> nanoparticles. We transform the modeled PDE's into ODE's by using similarity changes. Subsequently, we analyze impact of various parameters including the magnetic field parameter(*M*), prtial slip condition(*K*),

Eckert number( $Ec$ ), volume fraction( $\phi$ ), and nanoparticle Prandtl number ( $Pr$ ) on both the velocity and temperature profiles within the boundary layer. These effects are visually demonstrated through graphical results presented in figures 1.1 to 1.9.

Our study investigated the influence of various key parameters on the velocity profile of nanofluids containing different shapes of  $Al_2O_3$  nanoparticles. The results are presented visually in figures 1.1-1.4. Figures 1.1(a-e) Investigating the impact of the magnetic field parameter ( $M$ ) on the velocity profile within the boundary layer reveals a significant decrease in the velocity of all  $Al_2O_3$  nanoparticle shapes as  $M$  increases. This reduction can be attributed to Lorentz force generated by the interaction between applied magnetic field and the induced currents in the nanofluid. Figures 1.2(a-e) illustrate partial slip condition ( $K$ ) on the velocity profile shows that increasing  $K$  results in a reduction in velocity for all  $Al_2O_3$  nanoparticle shapes. This reduction can be explained by the decreased momentum transfer at the fluid-wall interface due to the partial slip condition. Figures 1.3(a-e) Investigating the effect of nanoparticle volume fraction ( $\phi$ ) on the velocity field reveals that increasing  $\phi$  generally enhances the velocity for most  $Al_2O_3$  nanoparticle shapes, including cylinders, platelets, blades, and bricks. However, an exception is observed with spherical nanoparticles, where an upsurge in  $\phi$  leads to a decline in velocity. This contrasting behavior is due to interplay of factors such as particle shape, interactions, and heat transfer mechanisms. Finally, figure 1.4 this analysis offers a fascinating comparison of the velocity profiles for different  $Al_2O_3$  nanoparticle shapes. The observed ranking of velocity from highest to lowest is platelets, cylinders, blades, bricks, and spheres. This suggests that platelet-shaped nanoparticles provide the greatest enhancement in nanofluid velocity, while spherical nanoparticles have the least impact.

In our study, we investigated not only the influence of various parameters on velocity profiles but also their impact on the thermal behavior of  $\text{Al}_2\text{O}_3$  nanofluid flows. Let's examine into the insights that were revealed by figures 1.5-1.9.

Figures 1.5(a-e) the interaction between the magnetic field parameter ( $M$ ) and fluid temperature is particularly intriguing. As  $M$  increases, there is a notable rise in fluid temperature. This phenomenon can be explained by the dissipation of kinetic energy into thermal energy, resulting from the Lorentz force acting on the electrically conducting nanofluid. Figures 1.6(a-e) the impact of the partial slip condition ( $K$ ) on temperature profile is also noteworthy. Interestingly, increasing  $K$  results in an increase in temperature for all  $\text{Al}_2\text{O}_3$  nanoparticle shapes. Figures 1.7(a-e) the effect of nanoparticle volume fraction ( $\phi$ ) on temperature is intriguing. Rising  $\phi$  generally leads to a temperature rise for most  $\text{Al}_2\text{O}_3$  nanoparticle shapes, including cylinders, platelets, blades, and bricks. This can be attributed to enhanced heat generation within the nanofluid due to the higher particle concentration. Figures 1.8(a-e) the role of the Eckert number ( $Ec$ ) in shaping the temperature profile is significant. As  $Ec$  increases, we observe a further rise in temperature. This indicates the increasing importance of viscous dissipation as fluid velocity increases. Finally, Figure 1.9 Our study presents a comparison of temperature profiles among different  $\text{Al}_2\text{O}_3$  nanoparticle shapes. We observe that the temperature ranking, from highest to lowest, is as follows: platelets, cylinders, blades, bricks, and spheres. This indicates that platelet-shaped nanoparticles have the most pronounced effect on heat generation, whereas spherical nanoparticles have the least impact. These findings uncover the complex relationships between various parameters and their influence on the thermal behavior of  $\text{Al}_2\text{O}_3$  nanofluids. Such insights are valuable for guiding the design and optimization of nanofluid-based systems across various applications in thermal management, energy harvesting, and beyond.



In Table.3 various values of different number like, volume fraction  $\phi$  and magnetic field M value of skin friction coefficient for different-shape  $Al_2O_3$  nanoparticles upsurge and for various values of skin friction coefficient and value of slip parameter K for multi-shape  $Al_2O_3$  nanoparticle decrease. In Table.4 Nusselt number is determined for different parameter like volume fraction  $\phi$ , magnetic field M and slip parameter K. It can be detected that value of Nusselt number decrease for various values of magnetic field M, Eckert number ( $Ec$ ), and volume fraction  $\phi$ , slip parameter K for multi-shapes of  $Al_2O_3$  nanoparticles.

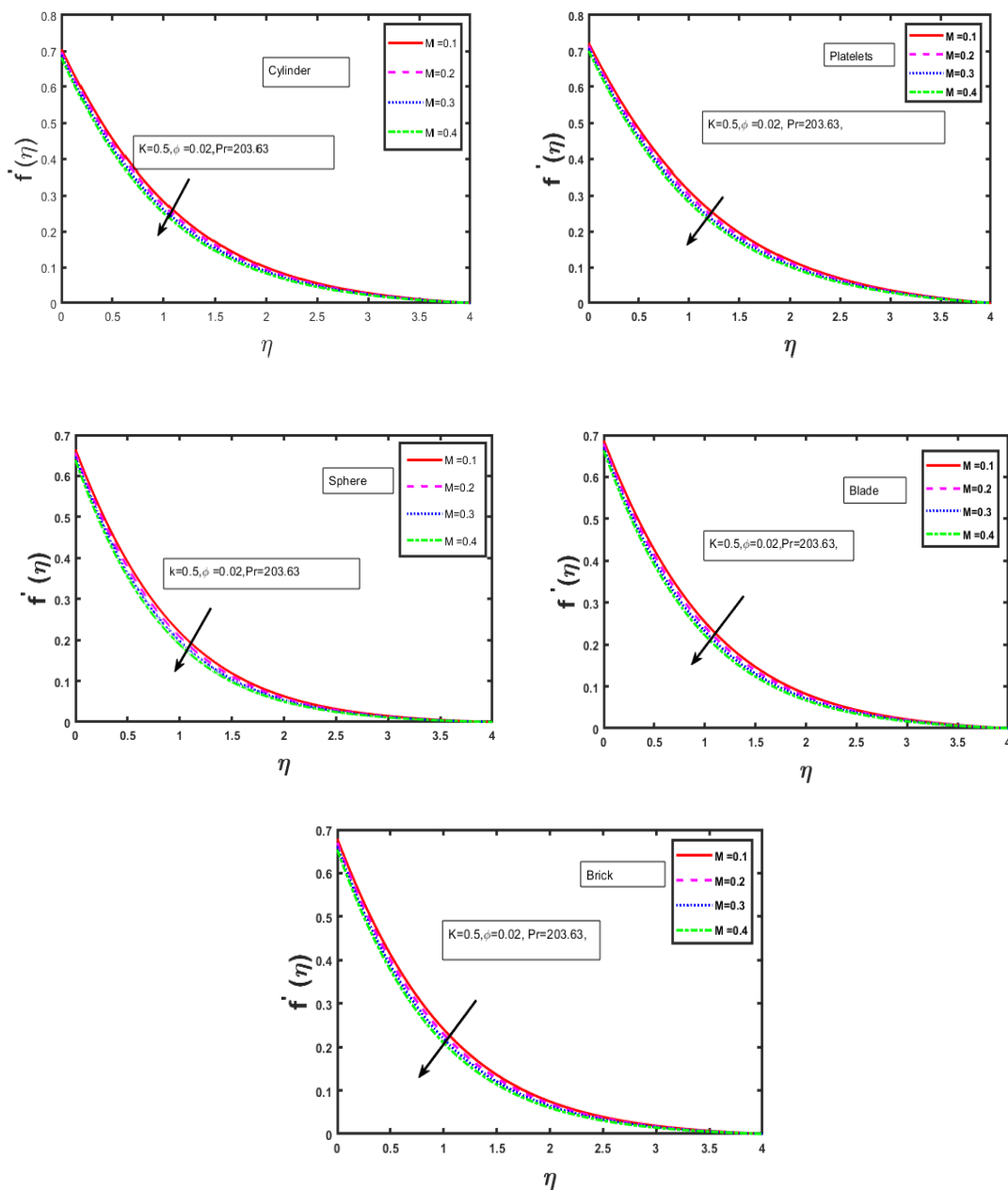


Figure 1.1(a-e): Effect of magnetic parameter ( $M$ ) on velocity profile.

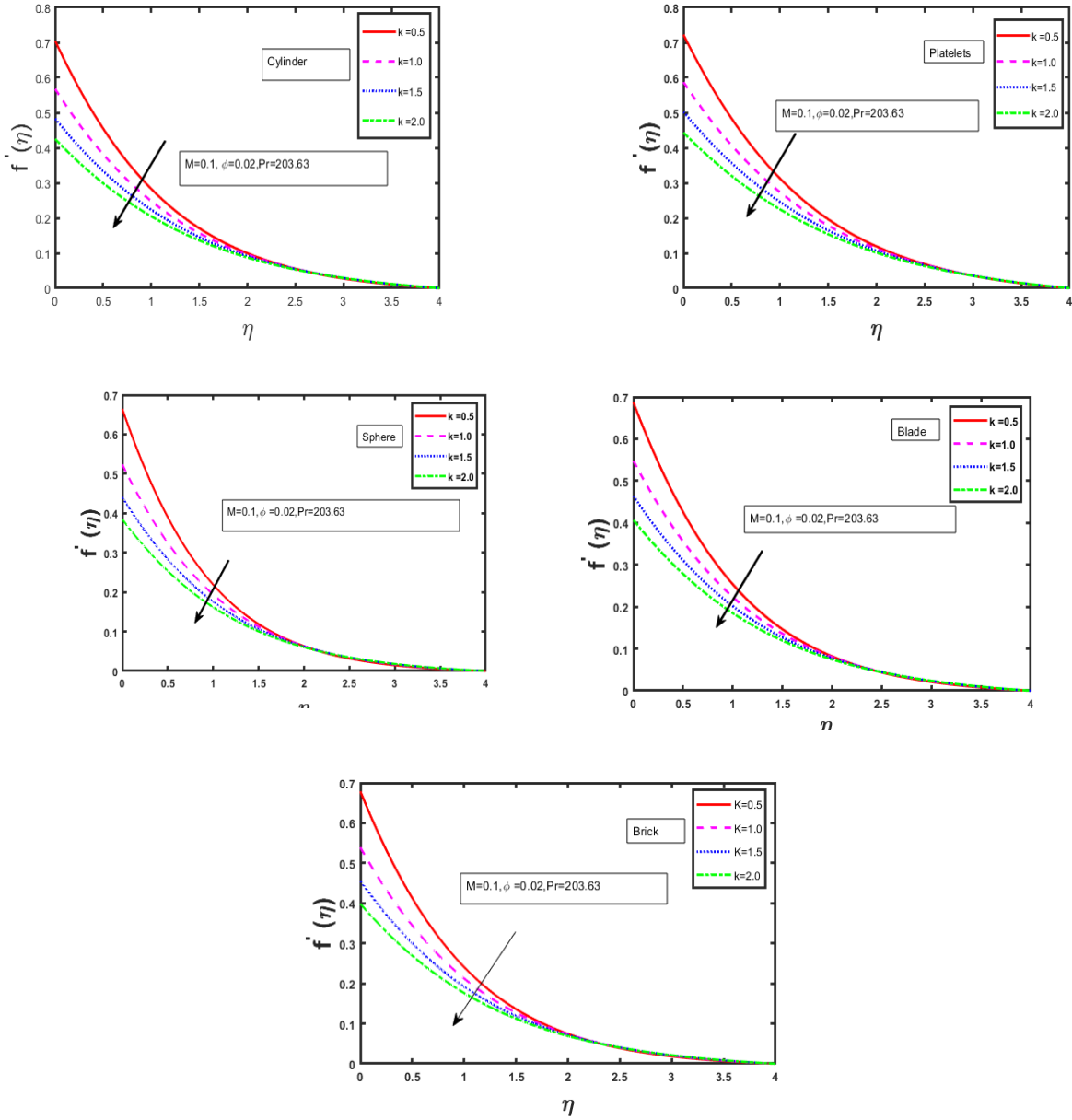


Figure 1.2(a-e): Outcome of Slip Parameter (K) on Velocity Profile.

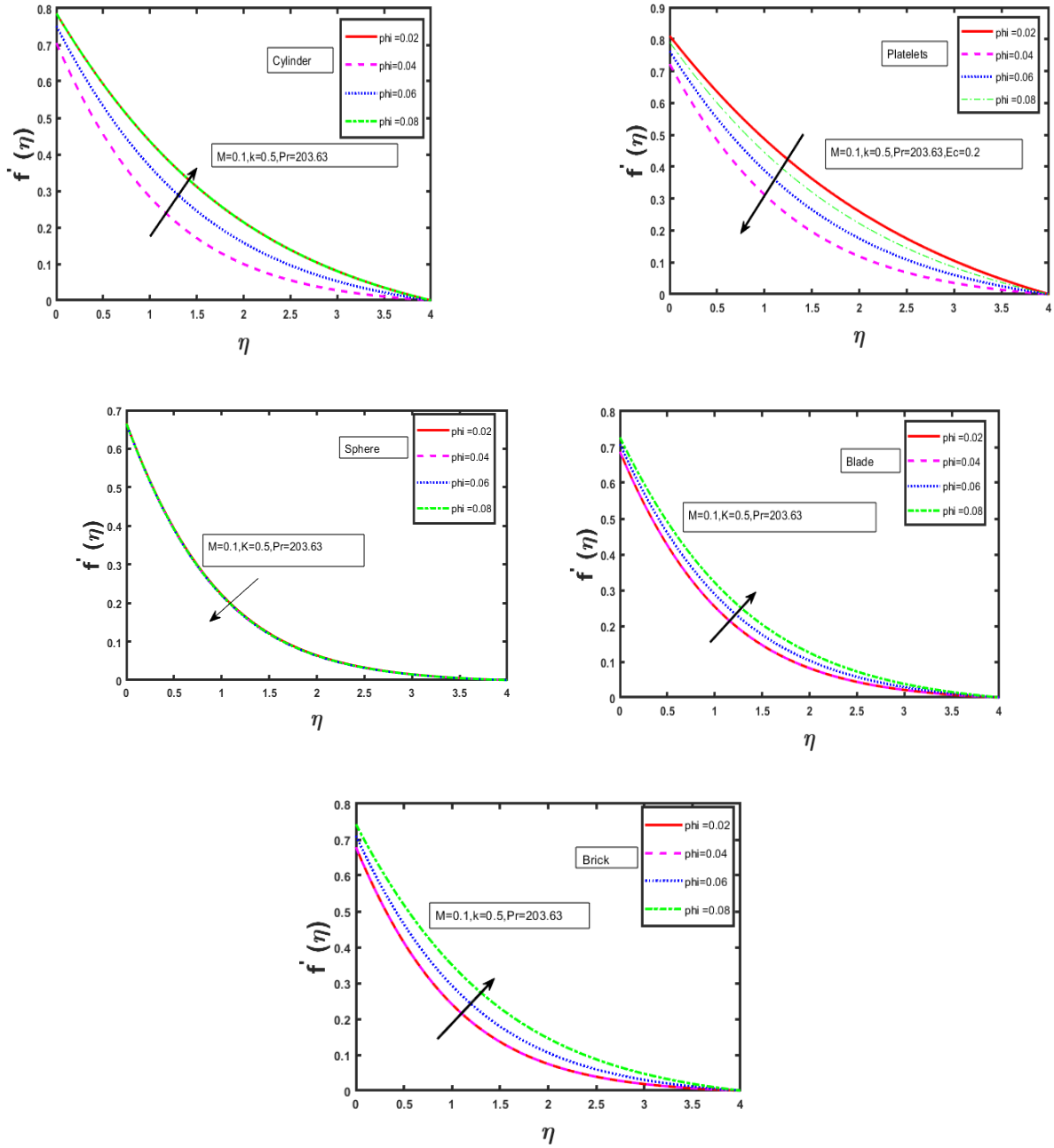


Figure 1.3(a-e): Influence on Volume Fraction ( $\phi$ ) on Velocity Profile.

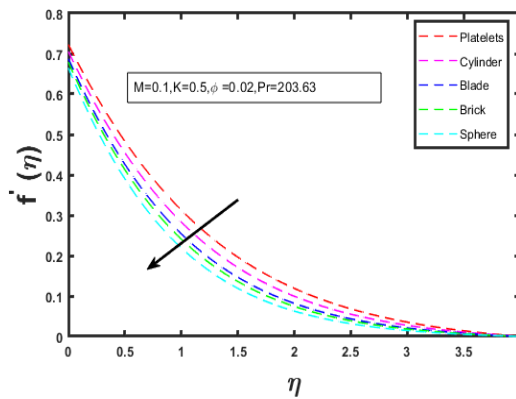


Figure 1.4. Dissimilarity in Velocity profile for Different shapes of nanoparticles.

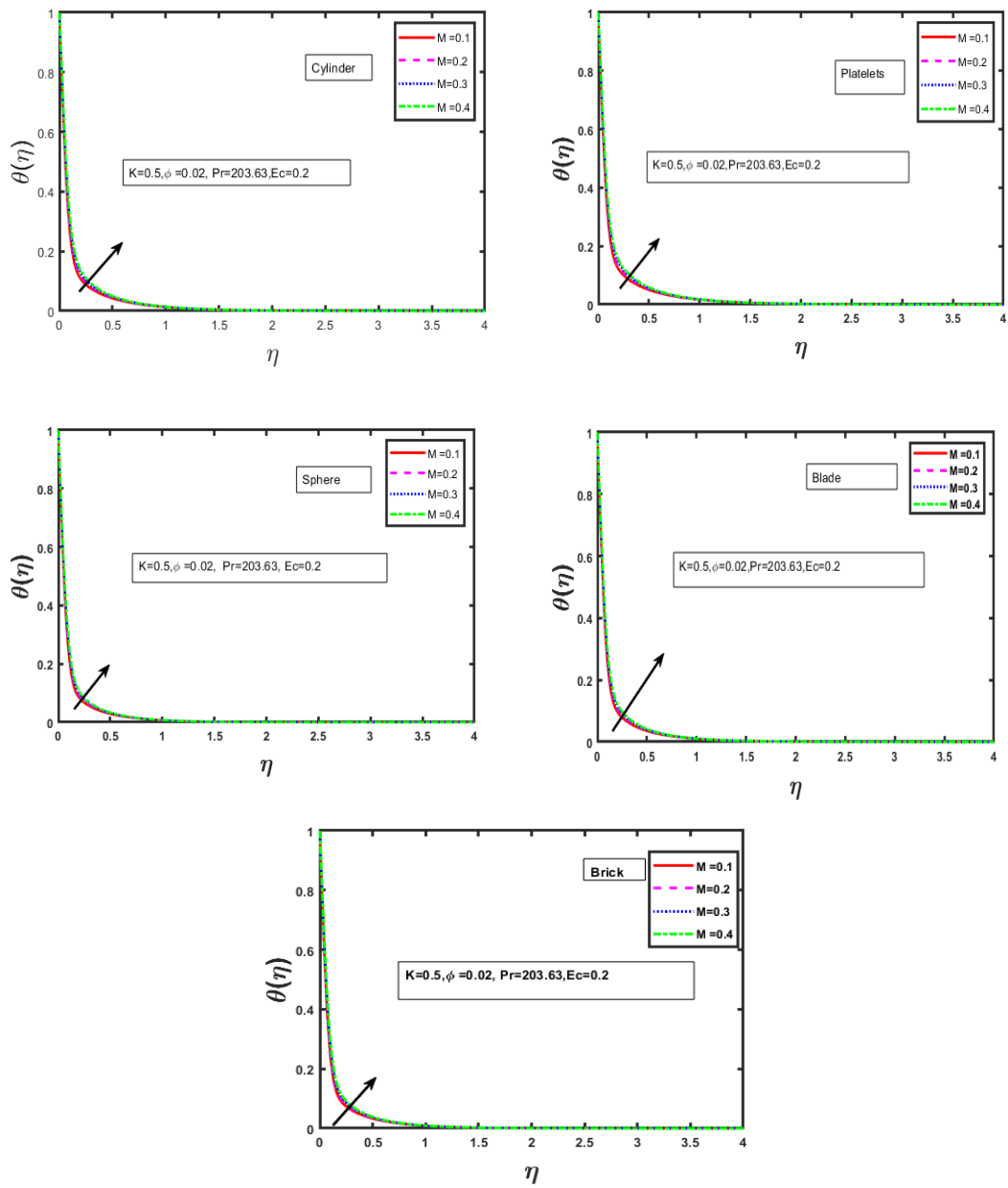


Figure 1.5(a-e): Influence of Magnetic Parameter (M) on Temperature Profile.

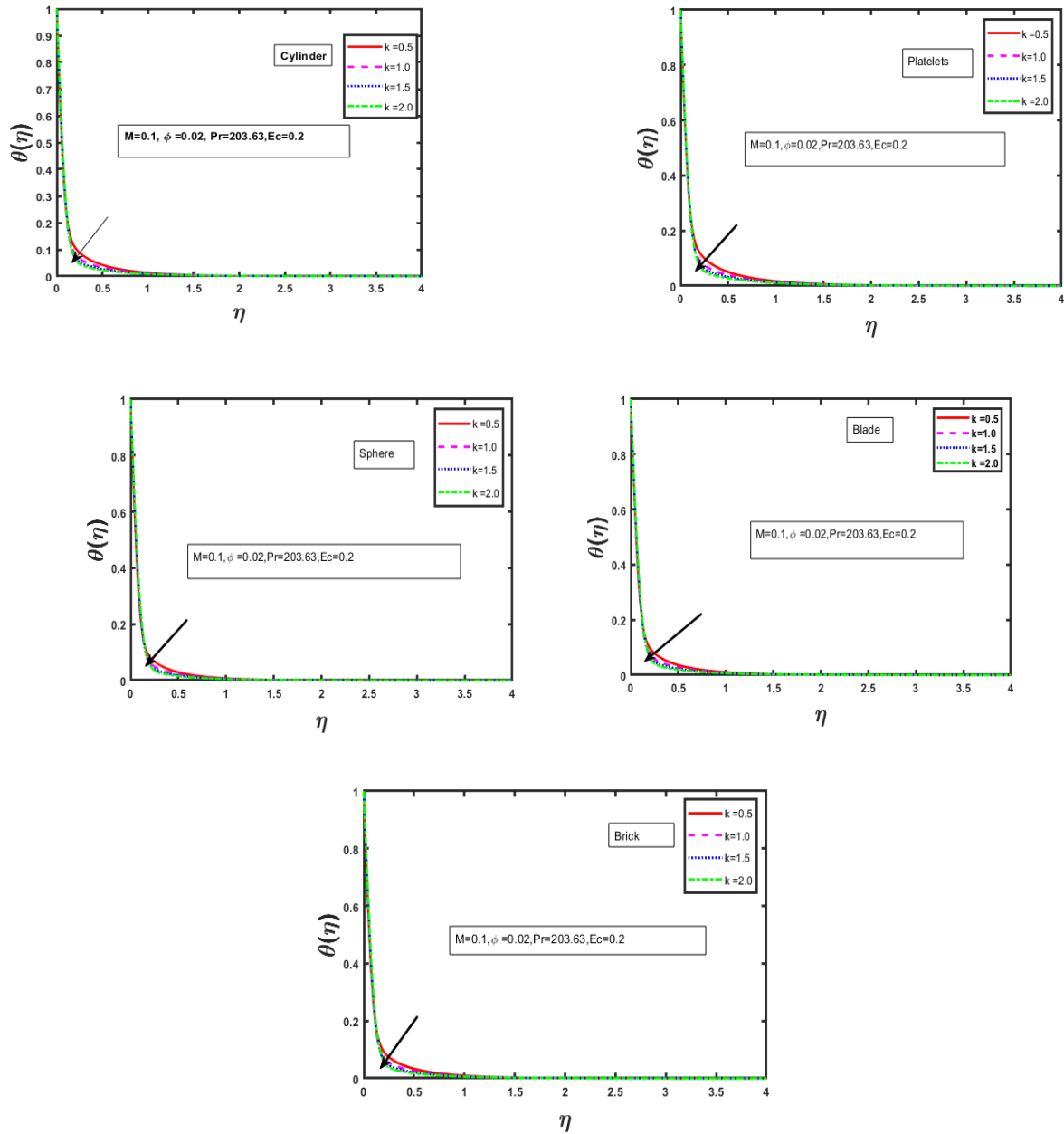


Figure 1.6(a-e): Influence of Slip Parameter (K) on Temperature

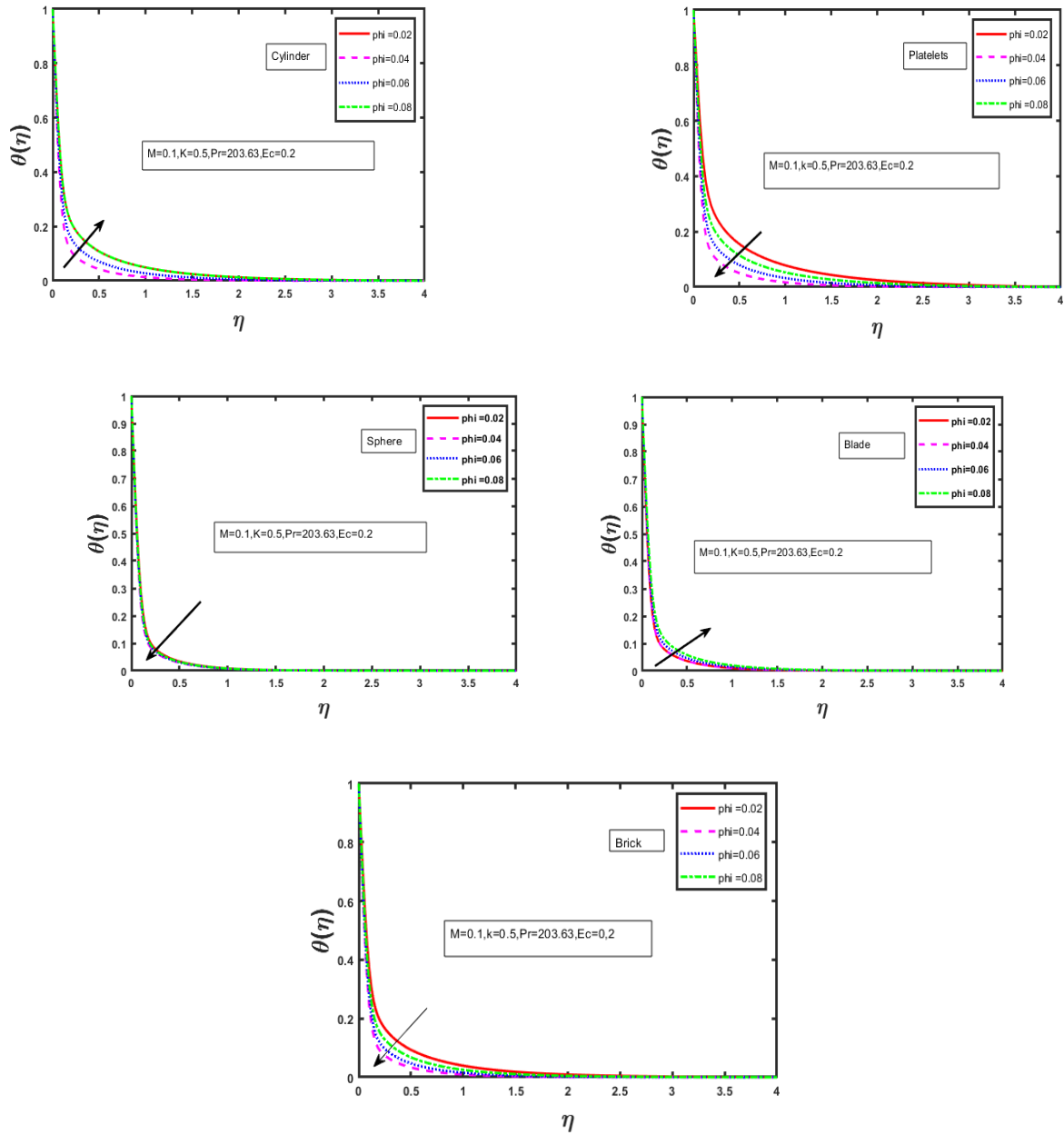


Figure 1.7(a-e): Influence of Volume Fraction Parameter ( $\phi$ ) on Temperature Profile.

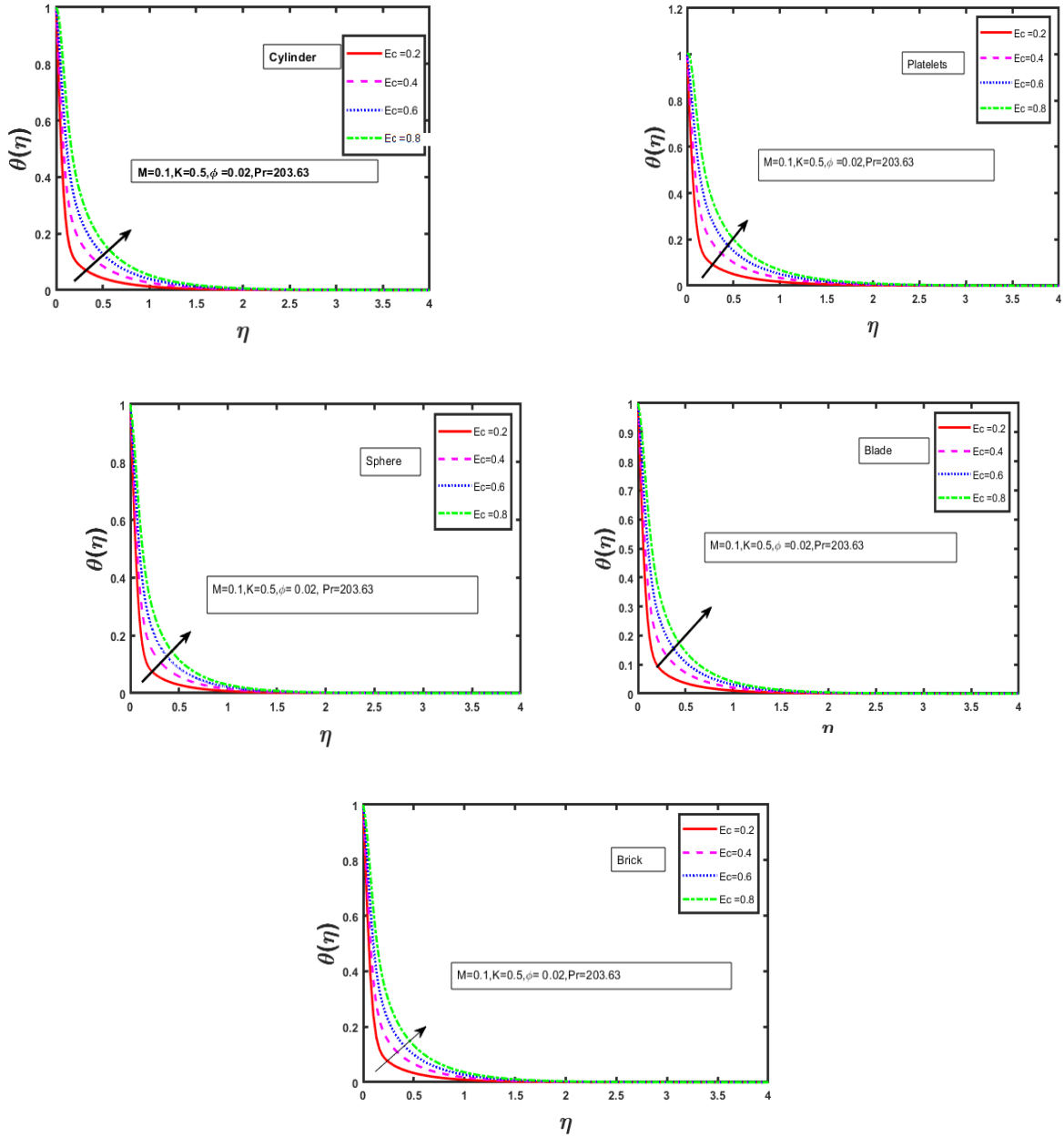


Figure 1.8(a-e): Influence of Eckert Number ( $Ec$ ) on Temperature

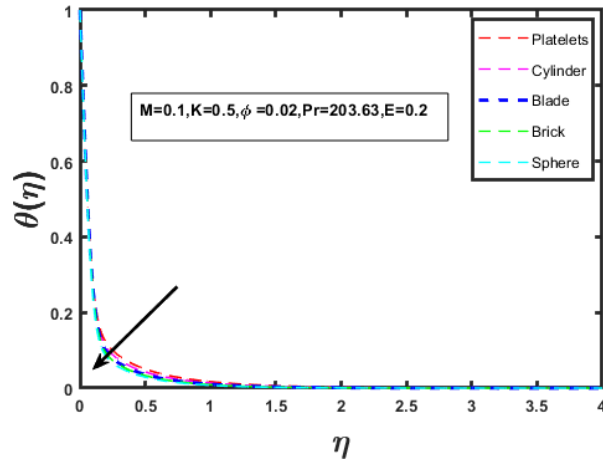


Figure 1.9. Dissimilarity on Temperature profile for Different shapes of nanoparticles.

**Table 3:** Numerical values of skin-friction coefficient of multi-shape nanoparticles.

<i>M</i>	<i>K</i>	$\phi$	$C_f Re^{\frac{1}{2}}$				
			Cylinder	Platelets	Sphere	Blade	Brick
0.1	0.5	0.02	-0.96224615	-1.1033513	-0.70617493	-0.83870587	-0.78735311
0.2	-	-	-0.98868052	-1.1335407	-0.72550429	-0.86175194	-0.80896765
0.3	-	-	-1.0139336	-1.1624625	-0.74385422	-0.88370633	-0.82953195
0.4	-	-	-1.0380806	-1.190193	-0.76129548	-0.90464273	-0.84911873
0.1	1.0	-	-0.70543935	-0.82064584	-0.50138444	-0.60610106	-0.56528219
-	1.5	-	-0.56190275	-0.65903261	-0.3923896	-0.47893582	-0.44508069
-	2.0	-	-0.4690514	-0.55310553	-0.3238174	-0.39771211	-0.36873806
-	0.5	0.04	-1.7614525	-1.9235574	-0.74495216	-1.1138058	-1.1748672
-	-	0.06	-2.5163371	-2.5751139	-0.78652079	-1.3525796	-1.625487
-	-	0.08	-3.3620693	-3.2990837	-0.83051285	-1.61335	-2.1424357

**Table 4:** Numerical values of Nusselt number of multi-shape nanoparticles.

<i>M</i>	<i>K</i>	<i>Ec</i>	$\phi$	$Nu Re^{-\frac{1}{2}}$				
				Cylinder	Platelets	Sphere	Blade	Brick
0.1	0.5	0.2	0.02	10.457017	10.373207	10.526912	10.926354	10.530832
0.2	-	-	-	9.9792611	9.866002	10.110353	10.465542	10.093397
0.3	-	-	-	9.5235222	9.3800512	9.7165047	10.02779	9.678608
0.4	-	-	-	9.0883088	8.9143233	9.343574	9.6113616	9.2846299
0.1	1.0	-	-	10.399926	10.438211	10.206279	10.727387	10.299828
-	1.5	-	-	10.081291	10.18996	9.7486813	10.322324	9.8872849
-	2.0	-	-	9.7292579	9.8799304	9.3187198	9.9146112	9.4816543
-	0.5	0.4	-	6.9414894	6.4768878	7.7522406	7.6834785	7.5108127
-	-	0.6	-	3.4259383	2.5805401	4.9775631	4.4405849	4.49081
-	-	0.8	-	-0.089647603	-1.3158206	2.2029636	1.1976633	1.4708638
-	-	0.2	0.04	10.457017	10.373207	10.526912	10.926354	10.530832
-	-	-	0.06	10.126187	10.04285	10.72121	11.39666	10.516259
-	-	-	0.08	9.3342773	9.36634	10.91265	11.743249	10.246441

**Conclusion**

Following conclusions draw from table that Al<sub>2</sub>O<sub>3</sub> nanoparticle under the following effects such as thermal radiation, joule heating, slip parameter , viscous dissipation magneto-hydrodynamic (MHD, over time independent radial stretching surfaces.



**Platelet-shaped nanoparticles:** These particles demonstrate rapid flow and heat transfer due to their elongated structure. Their shape allows for increased surface area, enhancing interaction with the surrounding fluid and promoting effective flow and heat exchange.

**Spherical nanoparticles:** Conversely, nanoparticles characterized by spherical shapes typically exhibit decreased rates of flow and heat transfer. Their smooth and symmetrical design limits the surface area in contact with the fluid, resulting in less effective heat and momentum transport.

**Nusselt number:** The Nusselt number, a dimensionless measure indicating heat transfer rate, diminishes as several factors increase. These factors include the magnetic parameter ( $M$ ), Eckert number ( $Ec$ ), slip parameter ( $K$ ), and volume fraction ( $\phi$ ) of nanoparticles. This suggests that these variables impede the nanofluid's capacity to efficiently transfer heat.

**Skin friction:** As the magnetic parameter ( $M$ ) and volume fraction ( $\phi$ ) increase, the magnitude of skin friction, indicating the viscous force on the fluid's surface, also increases, leading to a more pronounced drag force against the flow. Conversely, higher values of the slip parameter ( $K$ ) result in a reduction of skin friction, as the slip phenomenon enables the fluid to slide more effortlessly past the surface.

Continued advancements in the field will provide deeper insights into this intricate subject. Through exploring the interaction of diverse physical factors at the nano-scale, scientists can gain a better understanding of the complex relationship between nanoparticle flow, heat transfer, and Joule heating. This enhanced comprehension has the potential to drive the development of materials and technologies boasting remarkable thermal management capabilities.

## References

- [1]. Choi, S. U., & Eastman, J. A. (1995). Enhancing thermal conductivity of fluids with nanoparticles (No. ANL/MSD/CP-84938; CONF-951135-29). Argonne National Lab.(ANL), Argonne, IL (United States).
- [2]. Buongiorno, J. (2006). Convective transport in nanofluids.
- [3]. Ariel, P. D. (2007). Axisymmetric flow due to a stretching sheet with partial slip. *Computers & Mathematics with Applications*, 54(7-8), 1169-1183.
- [4]. Mustafa, M., Hayat, T., & Alsaedi, A. (2012). Axisymmetric flow of a nanofluid over a radially stretching sheet with convective boundary conditions. *Current Nanoscience*, 8(3), 328-334.
- [5]. Makinde, O. D., Mabood, F., Khan, W. A., & Tshehla, M. S. (2016). MHD flow of a variable viscosity nanofluid over a radially stretching convective surface with radiative heat. *Journal of Molecular Liquids*, 219, 624-630.
- [6]. Li, Z., Shafee, A., Kandasamy, R., Ramzan, M., & Al-Mdallal, Q. M. (2019). Nanoparticle transportation through a permeable duct with Joule heating influence. *Microsystem Technologies*, 25, 3571-3580.
- [7]. Hayat, T., Muhammad, T., Shehzad, S. A., & Alsaedi, A. (2017). On magnetohydrodynamic flow of nanofluid due to a rotating disk with slip effect: A numerical study. *Computer Methods in Applied Mechanics and Engineering*, 315, 467-477.
- [8]. Sarkar, G. M., Sahoo, B., & Bera, A. (2023). On dual solutions of an unsteady flow of Reiner-Rivlin fluid over a stretchable rotating disk with deceleration. *International Journal of Applied and Computational Mathematics*, 9(5), 97.
- [9]. Gangadhar, K., Kannan, T., Sakthivel, G., & DasaradhaRamaiah, K. (2020). Unsteady free convective boundary layer flow of a nanofluid past a stretching surface using a spectral relaxation method. *International journal of ambient energy*, 41(6), 609-616.
- [10]. Sandeep, N., Ranjana, B., Samrat, S. P., & Ashwinkumar, G. P. (2022). Impact of nonlinear radiation on magnetohydrodynamic flow of hybrid nanofluid with heat source effect. *Proceedings of the Institution of Mechanical Engineers, Part E: Journal of Process Mechanical Engineering*, 236(4), 1616-1627.
- [11]. Vinita, V., & Poply, V. (2020). Impact of outer velocity MHD slip flow and heat transfer of nanofluid past a stretching cylinder. *Materials Today: Proceedings*, 26, 3429-3435.
- [12]. Vinita, Poply, V., Goyal, R., & Sharma, N. (2021). Analysis of the velocity, thermal, and concentration MHD slip flow over a nonlinear stretching cylinder in the presence of outer velocity. *Heat Transfer*, 50(2), 1543-1569.
- [13]. Zaher, A. Z., Ali, K. K., & Mekheimer, K. S. (2021). Electroosmosis forces EOF driven boundary layer flow for a non-Newtonian fluid with planktonic microorganism: Darcy Forchheimer model. *International Journal of Numerical Methods for Heat & Fluid Flow*, 31(8), 2534-2559.
- [14]. S, Das & Sarkar, Flow analysis of Reiner-Rivlin fluid between two stretchable rotating disks. *Recent Trends in Wave Mechanics and Vibrations*, Springer, Singapore, 2020, pp. 61-70. Gangadhar, K., Kannan, T., Sakthivel, G., & DasaradhaRamaiah, K. (2020).
- [15]. Unsteady free convective boundary layer flow of a nanofluid past a stretching surface using a spectral relaxation method. *International journal of ambient energy*, 41(6), 609-616.
- [16]. Jiang, Y., Zhou, X., & Wang, Y. (2020). Effects of nanoparticle shapes on heat and mass transfer of nanofluid thermocapillary convection around a gas bubble. *Microgravity Science and Technology*, 32, 167-177.
- [17]. Gujar, J. G., Patil, S. S., & Sonawane, S. S. (2023). A Review on Nanofluids: Synthesis, Stability, and Uses in the Manufacturing Industry. *Current Nanomaterials*, 8(4), 303-318.
- [18]. Patil, P. M., & Shankar, H. F. (2022). Heat transfer attributes of Al<sub>2</sub>O<sub>3</sub>-Fe<sub>3</sub>O<sub>4</sub>/H<sub>2</sub>O hybrid nanofluid flow over a yawed cylinder. *Propulsion and Power Research*, 11(3), 416-429. Patil, P. M., & Benawadi, S. (2024). The mixed convection flow of a Williamson nanoliquid over a rotating sphere with the aspects of activation energy. *International Journal of Modelling and Simulation*, 44(1), 31-43.
- [19]. Patil, P. M., Shashikant, A., Hiremath, P. S., & Roy, S. (2019). Study of liquid oxygen and hydrogen diffusive flow past a sphere with rough surface. *International Journal of Hydrogen Energy*, 44(48), 26624-26636.
- [20]. Patil, P. M., Shankar, H. F., Hiremath, P. S., & Momoniat, E. (2021). Nonlinear mixed convective nanofluid flow about a rough sphere with the diffusion of liquid hydrogen. *Alexandria Engineering Journal*, 60(1), 1043-1053.

- [21]. Butt, A. S., Ali, A., & Mehmood, A. (2017). Hydromagnetic stagnation point flow and heat transfer of particle suspended fluid towards a radially stretching sheet with heat generation. *Proceedings of the National Academy of Sciences, India Section A: Physical Sciences*, 87, 385-394.
- [22]. Soomro, F. A., Haq, R. U., Al-Mdallal, Q. M., & Zhang, Q. (2018). Heat generation/absorption and nonlinear radiation effects on stagnation point flow of nanofluid along a moving surface. *Results in physics*, 8, 404-414.
- [23]. Nadeem, S., Ahmad, S., & Muhammad, N. (2018). Computational study of Falkner- Skan problem for a static and moving wedge. *Sensors and Actuators B: Chemical*, 263, 69-76.
- [24]. Rahman, J. U., Khan, U., Ahmad, S., Ramzan, M., Suleman, M., Lu, D., & Inam, S. (2019). Numerical simulation of Darcy–Forchheimer 3D unsteady nanofluid flow comprising carbon nanotubes with Cattaneo–Christov heat flux and velocity and thermal slip conditions. *Processes*, 7(10), 687.
- [25]. Bibi, S., Elahi, Z., & Shahzad, A. (2020). Impacts of different shapes of nanoparticles on SiO<sub>2</sub> nanofluid flow and heat transfer in a liquid film over a stretching sheet. *Physica Scripta*, 95(11), 115217.
- [26]. Khashi'ie, N. S., Arifin, N. M., & Pop, I. (2022). Magnetohydrodynamics (MHD) boundary layer flow of hybrid nanofluid over a moving plate with Joule heating. *Alexandria Engineering Journal*, 61(3), 1938-1945.
- [27]. Saleem, S., Qasim, M., Alderremy, A., & Noreen, S. (2020). Heat transfer enhancement using different shapes of Cu nanoparticles in the flow of water based nanofluid. *Physica Scripta*, 95(5), 055209.
- [28]. Shampine, L. F., Kierzenka, J., & Reichelt, M. W. (2000). Solving boundary value problems for ordinary differential equations in MATLAB with bvp4c. *Tutorial notes*, 2000, 1-27.
- [29]. Hayat, U., & Shahzad, A. (2023). Analysis of heat transfer and thin film flow of Au– Np over an unsteady radial stretching sheet. *Numerical Heat Transfer, Part A: Applications*, 84(11), 1338-1351.